Ceramics International 44 (2018) 15092–15098

Contents lists available at ScienceDirect

Ceramics International

journal homepage: www.elsevier.com/locate/ceramint

Reduced graphene oxide and ZnO decorated graphene for biomedical applications

P.K. Sandhya[a], Jiya Jose[b], M.S. Sreekala[c], M. Padmanabhan[a,d], Nandakumar Kalarikkal[b], Sabu Thomas[a,*]

[a] School of Chemical Sciences, M.G. University, Kottayam 686560 Kerala, India
[b] International and Inter University Centre for Nanoscience and Nanotechonology, M.G. University, Kottayam 686560 Kerala, India
[c] Post Graduate Department of Chemistry, Sree Sankara College, Kalady 683574, Kerala, India
[d] Department of Chemistry, Amrita Vishwa Vidyapeetham, Amritapuri, 690525 Kerala, India

ARTICLE INFO

Keywords:
Potato starch
Reduced graphene oxide
ZnO-RGO
Antibacterial activity

ABSTRACT

The ability of graphene-based materials to enhance the conventional antibiotic resistance is well known and researchers have been interested in improving their antibacterial activity. The reduction of graphene oxide by eco-friendly reducing agents is of great interest on the basis of environmental and human health aspects. Herein we report the synthesis of two forms of graphene derivatives namely, reduced graphene oxide (RGO) through reduction using potato starch and zinc oxide decorated RGO (ZnO-RGO). In the case of ZnO-RGO, the reduction of graphene oxide and the conversion of ZnO to nano ZnO occur simultaneously. The characterization of all the graphene based materials and nanocomposites developed were carried out using FT-IR, XRD, Raman spectra and TEM techniques. The antibacterial activity of these modified materials against *E. coli* was also studied by well diffusion method. Our results show that ZnO-RGO is more efficient than RGO in their antibacterial properties which we attribute to the synergistic effect of ZnO and RGO towards the bacteria in the nanocomposite. Further we find that the antibacterial effect of ZnO-RGO towards *E. coli* is due to the disruption of the bacterial cell which could be confirmed by AFM images. Considering the fact that graphene-based materials are less toxic towards mammalian cells, both RGO and ZnO-RGO we have developed can find applications in the field of medicine and life sciences.

1. Introduction

The emergence of multiple drug-resistant human pathogens is a major problem faced by present world due to the widespread and inappropriate use of antibiotics. Hence it is very important to develop new and effective antimicrobial agents with suitable biocompatibility and showing a broad spectrum of bactericidal activity [1,2]. Among the carbon based nanomaterials, graphene derivatives have emerged as a new antibacterial material because of its less cytotoxicity towards mammalian cells as compared to carbon nanotubes and diversity in their bactericidal activities [3]. Graphene can perform its antibacterial activity both through its physical and chemical effects. Direct contact of sharp edges of graphene sheets with bacterial membranes, destructive extraction of lipid molecules, wrapping and photo-thermal ablation mechanisms are involved in the physical effects. The oxidative stress caused by the reactive oxygen species (ROS) and charge transfer features are involved in chemical effects [3]. Applications of graphene-based materials in the field of medicine and life sciences especially for pathogen control [4], imaging [5], drug delivery [6] and biosensors [7] have been well demonstrated.

Graphene, which is a two-dimensional material consisting of a single atomic layer of sp^2 hybridized carbon atoms arranged hexagonally, is a very unique material known for its versatile properties [8,9]. Graphene and its derivatives serve as nanoscale building blocks for composite antibacterial materials because of its outstanding physical properties, water solubility, high specific surface area and plenty of reactive surface functionalities [10]. Methods used for the production of graphene are mostly micromechanical cleavage [11,12], chemical vapor deposition [13,14], chemical exfoliation [15,16], liquid phase exfoliation assisted by ultrasonication [17,18]. The most widely used reducing agent for the reduction of graphene oxide to its reduced form (RGO) is hydrazine monohydrate [19]. But the presence of even trace amount residual hydrazine can affect the performance of RGO based systems. Moreover, it is highly toxic and dangerously unstable. Several environmentally friendly high-efficiency reducing agents have been developed which are used as an alternative to hydrazine. The most

* Corresponding author.
E-mail address: sabuthomas@mgu.ac.in (S. Thomas).

https://doi.org/10.1016/j.ceramint.2018.05.143
Received 13 March 2018; Received in revised form 14 May 2018; Accepted 16 May 2018
Available online 17 May 2018

commonly used eco-friendly reducing agents are reducing sugar [20], alcohols [21], vitamin C [22], tea [23] and reducing metal powders [24].

The stacking of graphene layers through collective van der Waals forces can affect bactericidal performance but it can be reduced by introducing nanoparticles or molecular units which prevent the re-stacking of layers [9]. But anchoring the GO sheets with metal or metal oxide nanoparticles directly or indirectly can be a better strategy as it can enhance its properties [25–27]. The appreciable interest of ZnO over other semiconductors is due to its low cost, ease of availability, size, and shape-dependent photocatalytic properties and its applications in many fields such as gas sensors, photocatalysis, photodetectors, solar cells, electrochemical sensing, etc. Moreover, the smaller size of ZnO provides a large surface area and more active surface sites when the absorbed molecules interact with the photogenerated charge carriers to form hydroxyl and superoxide radicals [28]. The enhanced bioactivity of ZnO is well known, and it is considered as a 'generally recognized as safe' (GRAS) material. It also shows minimal effects on human cells which makes it useful in food industry [29].

The antibacterial activity of graphene oxide (GO) and RGO were first reported by Fan and Haung, who found that graphene-based nanomaterials can effectively inhibit the growth of *E. coli* with minimum cytotoxicity [30]. Nanda and colleagues studied the antibacterial activity and proposed underlying mechanism of GO against *E.coli* and *Enterococcus faecalis* by a new and sensitive fingerprint approach using Raman spectroscopy [31]. Liu et al. [32] compared the antibacterial activity of four types of graphene based materials such as graphite (Gt), graphite oxide (GtO), graphene oxide (GO) and reduced graphene oxide (rGO) against *E.coli* and they found that the order of antibacterial activity is GO > rGO > Gt > GtO. Krishnamoorthy and colleagues studied the antibacterial activity of GO towards Gram-negative bacteria '*E.coli*' and Gram-positive bacteria '*Streptococcus iniae*' by the colony counting method and found that GO shows more activity towards Gram-positive bacteria [33]. Electron spin resonance (ESR) technique coupled with spin-trapping technique was used for confirming the underlying mechanism of the antibacterial activity. Kellici and co-workers synthesized RGO with antibacterial activity in a single rapid route by utilization of continuous supercritical water in alkaline medium without using any hazardous conventional chemicals [34]. Several reports demonstrated the antibacterial activities of RGO, tungsten disulphide (WS_2) and reduced graphene oxide-tungsten disulphide (RGO-WS_2) by time and concentration-dependent viability assay against four different bacterial strains [35]. They found that RGO-WS_2 showed significant retardation in bacterial growth and inhibitory effect compared to others. Ravichandran and colleagues successfully prepared cobalt activated ZnO nanocomposites on the surface of reduced graphene oxide (ZnO:Co/RGO) by a simple cost-effective method and studied the photocatalytic and antibacterial activities [36]. They found that ZnO:Co/RGO showed improved antibacterial activity against *S.aureus* and *E.coli*. Studies on a simple and facile one-pot chemical approach for the preparation of ZnO on graphene oxide and the antibacterial activity of RGO-ZnO composites against *E.coli* were also reported in which RGO-ZnO was shown to be having pronounced antibacterial activity than pure RGO [29].

In the present study, we report the preparation of GO from graphite powder by Hummer's [37] method and carry out a very effective reduction of GO to RGO using potato starch as reducing agent which is highly eco-friendly and abundantly available [38]. Another graphene-based material we have developed is a new form of RGO-ZnO nanocomposite which is formed from GO by chemically decorating its surface with ZnO [39]. Interestingly in this case we find that both the reduction of GO to RGO and the conversion of ZnO to nano-ZnO simultaneously. The antibacterial activity of these graphene derivatives was studied against *E.coli* by well diffusion method. The cell wall integrity analysis using SDS assay and AFM image of *E.coli* was also used for confirming the effect of graphene nanoparticles on *E.coli*. To understand the mode of action of graphene nanoparticles and their bactericidal properties on *E.coli* both SDS assay and AFM imaging were carried out from which we could confirm the cell wall disruption as the main reason.

2. Experimental

2.1. Materials

Graphite powder, sodium nitrate ($NaNO_{3)}$, concentrated sulphuric acid (conc. $H_2SO_{4)}$, potassium permanganate ($KMnO_4$), hydrogen peroxide (H_2O_2), ammonia, N,N-dimethylformamide (DMF), zinc acetate dihydrate ($Zn(CH_3COO)_2{\cdot}2H_2O$) were purchased from Merck, India. Potato starch was procured from (LOBA Chemie Pvt. Ltd). Gram- negative *Escherichia coli* were used for the antibacterial study.

2.2. Preparation of GO

The preparation of GO was carried out by Hummers method on graphite powder using, an oxidation process. In this process, 5 g natural graphite and 2.5 g of $NaNO_3$ were mixed and added to an ice-cooled 115 mL of conc. H_2SO_4 by continuous stirring. About 15 g of $KMnO_4$ was added to this solution within 1 h. After adding 230 mL of distilled water carefully, the reactants were heated to 35 °C and stirred for 30 min. The temperature of the reaction mixture was raised to 80 °C and maintained at that temperature for 45 min. The reaction was completed by adding 700 mL of distilled water and 30% aqueous solution of 12.5 mL of H_2O_2. The resulting solution was washed several times with distilled water, until the filtrate showed neutral pH. The resulting solution was sonicated for 5 min and dried at 60–65 °C in an oven.

2.3. Preparation of RGO

Reduction of GO to RGO was carried out using abundantly available potato starch as the reducing agent. About 0.2 g of potato starch was added to 125 mL of GO dispersion (0.5 mg/mL) in distilled water which was then subjected to stirring for about 30 min. About 25% ammonia solution was added to the reaction mixture to adjust the pH in the range 9–10. The reaction mixture was refluxed at 80 °C for 3 h by continuous stirring and then allowed to cool. The product was washed several times with distilled water until the filtrate is free from alkali. The product obtained was dried at 30 °C for further use.

2.4. Preparation of ZnO-RGO

GO (0.04 g) was uniformly dispersed in 120 mL of DMF by sonication for 30 min. Zinc acetate dihydrate (0.92 g) was dissolved in 120 mL DMF and added to GO solution and stirred for 30 min. The reaction mixture was then subjected to heating at 95 °C for 5 h with continuous stirring and cooled to room temperature. It was then washed with ethanol to remove the traces of DMF and dried at 60 °C. For the synthesis of blank ZnO, the procedure was the same as the one used for ZnO-RGO but without the addition of GO. Shown in Scheme 1 are the steps involved in the preparation of RGO and ZnO-RGO.

2.5. Characterization

Fourier transform infrared (FT-IR) spectrum of graphite powder, GO and RGO were measured on a PerkinElmer Spectrum 400 model automatic IR spectrometer with attenuated total reflectance (ATR) mode between the frequency ranges of 4000–500 cm^{-1}. The XRD measurements were carried out using an X-ray diffractometer XPERT-PRO and the intensity were recorded in 2θ range 5–40° with step size 2θ at 0.001 using a Ni-filtered Cu K_α radiation (θ = 1.5406 Å) and an operating voltage of 45 kV and a filament current of 35 mA. The morphological analysis of the prepared nanoparticles was obtained on a High-

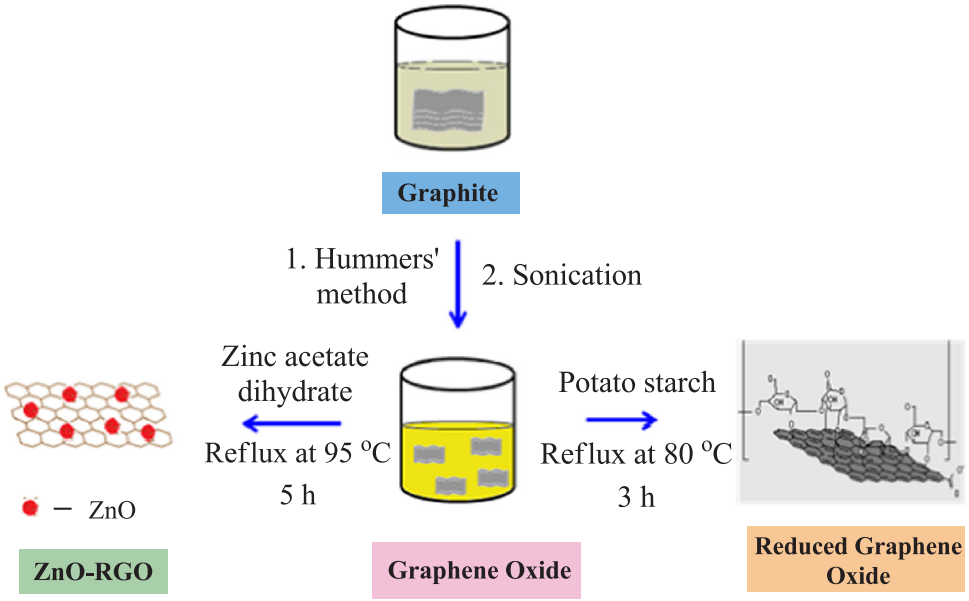

Scheme 1. Steps involved in the preparation of RGO and ZnO-RGO.

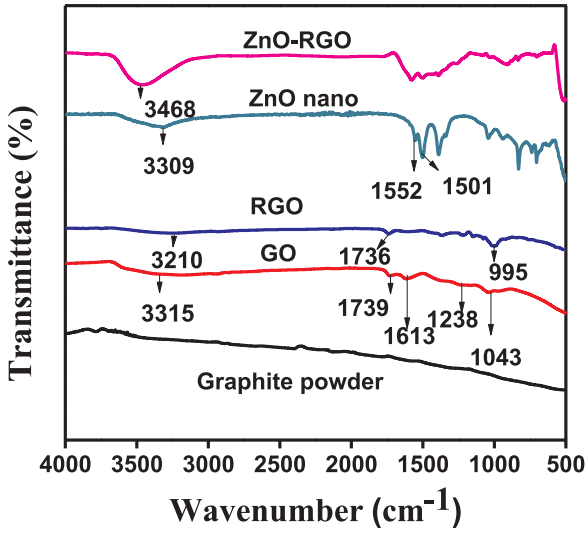

Fig. 1. FT-IR spectra of graphite, GO, RGO, ZnO nano and RGO-ZnO.

Resolution Transmission Electron Microscope JEM-2100HRTEM. The Raman spectra of the samples were done in WITec Alpha 300 RA confocal Raman microscope with AFM (WITec GmbH, Ulm, Germany).

2.6. Antibacterial activity of RGO and ZnO-RGO

The antimicrobial activity of the powder samples were assessed using the well diffusion method. Nutrient agar was poured into the assay plate and allowed to cool down. Once the medium is solidified, wells each of 1 cm in diameter were cut out of the agar, and 50 µL of the sample solution RGO and ZnO-RGO respectively were placed into each well. After 24 h incubations Zone of inhibition were measured.

2.7. Cell wall integrity using SDS (sodium dodecyl sulphate) treatment assay

The effect of various graphene nanoparticles on cell wall integrity of *Escherichia coli* was investigated by SDS assay following the method of Lok et al. [40]. Briefly, overnight cultures of bacterial cells were washed copiously with sterile phosphate buffered saline (8 g NaCl, 0.2 g KCl and 1.44 g KH_2PO_4 prepared in distilled water 1 L, pH 7.4) and dispensed in the wells of a sterile microplate to a volume of 200 µL. After measuring the initial absorbance, the test solution was supplemented with graphene nanoparticles (100 µg/mL) and SDS (0.1%). Control wells without graphene nanoparticles were maintained. The absorbance at 600 nm was recorded in every 15 min for a period of 2 h. Time versus cell wall integrity was then plotted.

2.8. Cell wall integrity analysis by Atomic Force Microscopy (AFM)

The cell wall integrity of *E. coli* was also studied by AFM experiments performed in contact mode using A.P.E.R research nanotechnology. In a typical experiment a drop of the suspension of *E. coli* after treating with RGO (2 µg/mL) in distilled water and control was applied separately on the surface of silica wafers and dried well before imaging.

3. Results and discussion

3.1. Characterization of RGO and ZnO-RGO

Fig. 1 represents the FT-IR spectrum of graphite, GO, RGO, ZnO-RGO and nano- sized ZnO. In the case of graphite powder, no significant peak was observed. For GO, a broad peak is observed at 3315 cm^{-1} corresponding to OH stretching. The peak observed at 1043 cm^{-1} and 1739 cm^{-1} represent C-O stretching vibration and C=O stretching vibration respectively. The peak at 1613 cm^{-1} represents un-oxidized graphitic domains and 1238 cm^{-1} for C-OH stretching vibrations [41]. These observed peaks are characteristic of GO formed from graphitic powder because of the presence of various functional groups present on GO during the exfoliation process. The intensity of O-H stretching vibrations observed at 3315 cm^{-1} was significantly reduced in the case of potato starch reduced graphene oxide which confirmed the reduction of GO and formation of RGO. The peak at 995 cm^{-1} indicates the C-O stretching and a peak at 1736 cm^{-1} indicate the C=O stretching. Theses observed peaks in RGO also indicate the presence of residual organic moieties originating from the starch units on the graphene surface as functional groups. In the case of ZnO-RGO the broad peak observed at

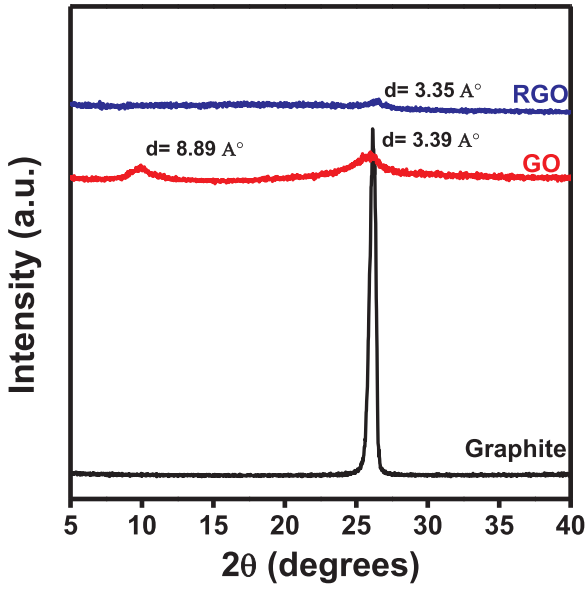

Fig. 2. XRD patterns of graphite, GO and RGO.

3468 cm^{-1} represents the –OH stretching vibration. The peaks at 1739 cm^{-1} and 1043 cm^{-1} in GO are absent due to the anchoring of ZnO on the graphene sheet [42]. The peaks observed at 1552 cm^{-1} and 1501 cm^{-1} correspond to the anti-symmetrical and symmetrical stretching of zinc carboxylate in the case of ZnO nano. The peak corresponding to the stretching vibration of ZnO bonds is observed at 473 cm^{-1}.

Fig. 2 displays the XRD patterns of graphite powder, GO and RGO. Graphite shows a sharp peak at 26.25° with a d-spacing of 3.39 Å. In the case of GO, a peak observed at 9.95° with a d-spacing of 8.89 Å which we attribute to the introduction of oxygenated functional groups on the surface of carbon sheet. There is also a peak at 26.26° corresponding to the partial oxidation of the carbon sheet. After reduction, the peak at 9.95° disappears and gets shifted to higher 2θ angles at 26.53° with a d-spacing of 3.35 Å [43]. The XRD results obtained indicate that GO is getting reduced successfully by potato starch and, further, the exfoliation also occur if any multilayered RGO is formed.

Fig. 3 represents the XRD patterns of ZnO nano and ZnO-RGO. The sharp diffraction peaks obtained clearly indicate the crystalline nature of ZnO particles formed on both cases, especially in the case of ZnO-RGO. The major peaks observed at 2θ = 31.82, 34.47, 36.48, 47.53,

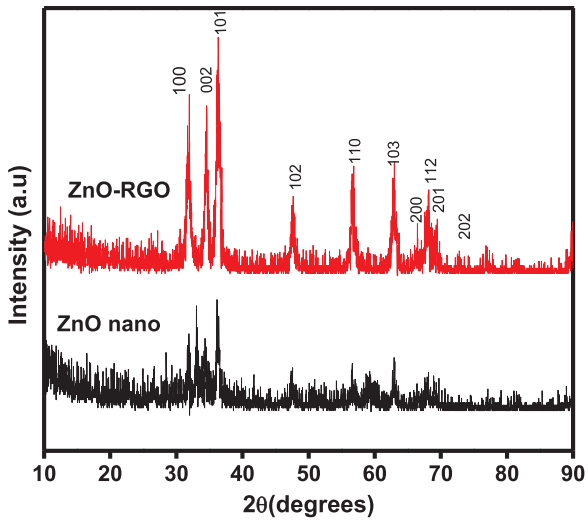

Fig. 3. XRD patterns of ZnO nano and ZnO-RGO.

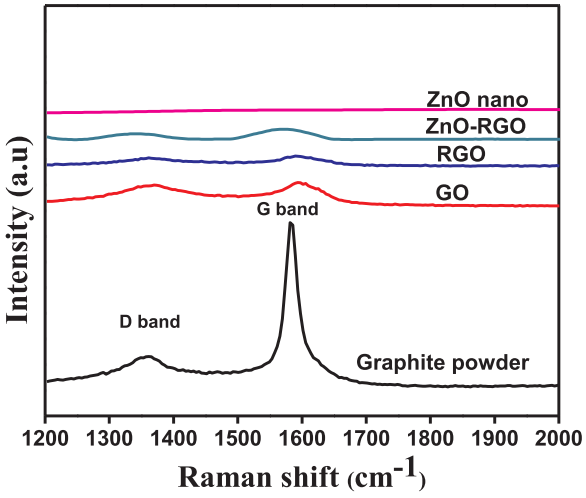

Fig. 4. Raman spectra of graphite, GO, RGO, ZnO nano and ZnO-RGO.

56.68, 62.94, 66.35, 67.97, 69.31, 72.77, 77.01 could be indexed which correspond to the lattice planes (100), (002), (101), (102), (110), (103), (200), (112), (201), (044), (202) respectively which clearly reveal that the synthesized nanoparticles have ZnO in its pure phase and possess a very high crystallinity. The peaks corresponding to GO (Fig. 2) are absent in ZnO-RGO indicating that GO was getting reduced to RGO during the formation of ZnO nano and layer stacking is prevented in the samples [39]. It also proves that the aggregation of graphene layers again into graphite is getting prevented by the presence of ZnO nano anchored on the surface of graphene sheets.

One of the important tools for the structural investigation of carbon materials is Raman spectra. The out-of-plane breathing mode of sp^2 atoms in graphite represents D band and the G band corresponds to the vibrations of sp^2 carbon atom domains of graphite. The graphite powder shows a D band at 1361 cm^{-1} and G band at 1582 cm^{-1}. Fig. 4 displays the Raman spectra patterns of graphite powder, GO, RGO, ZnO nano and ZnO-RGO obtained in the spectral range from 1200 to 2000 cm^{-1}. After oxidation, GO shows a D band at 1369 cm^{-1} indicating the reduction in the size of the sp^2 domains and a G band at 1593 cm^{-1} due to the presence of isolated double bonds resonating at higher frequencies than that of G band of graphite. RGO shows a D band at 1361 cm^{-1} and a G band at 1589 cm^{-1}. The ratio of peak intensities of D band and G band (I_D/I_G) is a measure of defects on graphene sheets and after reduction of GO, the I_D/I_G value increases from 0.9836 to 0.9865 indicating that most of the oxygenated groups GO is getting removed during reduction leading to partial ordering to crystalline form of graphene. The increase in I_D/I_G ratio of RGO obtained by green reducing methods was also reported elsewhere [38,44,45].

The defects in the graphitic structure correspond to the D band and the vibrations of sp^2 hybridized carbon atoms are to the G band [46]. In the case of ZnO-RGO, spectra show a shift in two bands, D band at 1345 cm^{-1} and G band at 1573 cm^{-1}. In the case of ZnO nano, no characteristic band is observed in the range of 1200–2000 cm^{-1}. The ratio of peak intensities of D band G band (I_D/I_G) provides information about the structure ordering (graphitization) of materials. After the treatment, the I_D/I_G value decreased from 0.9836 for GO to 0.9137 for ZnO-RGO. This suggests that in addition to the reduction of GO the aromatic structures are getting recovered by repairing defects [47]. Such a decrease in I_D/I_G value was also reported elsewhere [47,48]. While anchoring in situ formed nano ZnO on the surface of GO, a decrease in the contents sp^2 domains of carbon atoms occur which leads to a decrease in I_D/I_G value [49].

From the TEM image shown in Fig. 5(a), it is clear that some scrolling and corrugations occur on the edges of RGO. The RGO nanosheets are the layer structured, irregular and folded with lots of

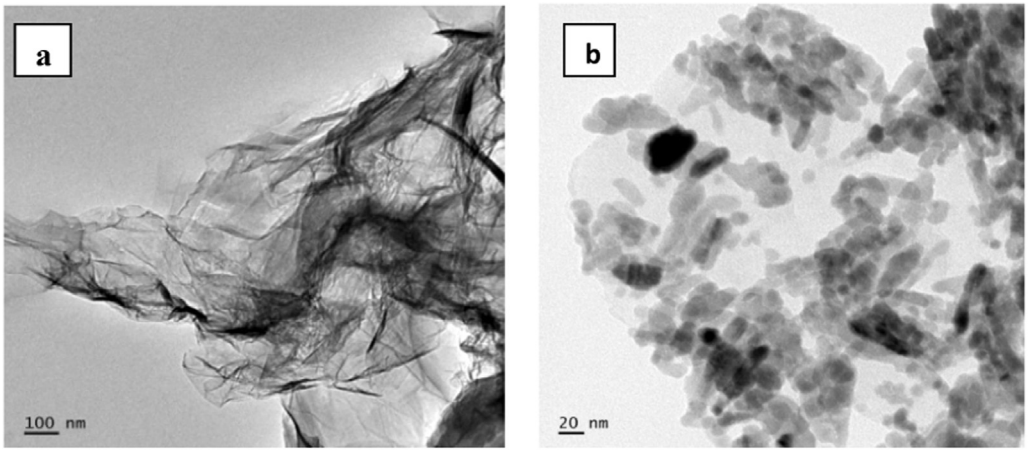

Fig. 5. TEM images of (a) RGO (b) ZnO-RGO.

wrinkles. From the image shown in Fig. 5(b), it can be seen that the light gray coloured domains represent the sheets of GO and the dark coloured domains on the surface of GO represent the ZnO nanoparticles. The wrinkled morphology of graphene layers also can be facilitating the antibacterial activity by trapping the bacteria which we confirm in our antibacterial studies. Further, it also confirms that the in situ generated form of ZnO is in nano-form uniformly and is getting decorated through anchoring on the layer surfaces of RGO.

3.2. Antibacterial activity

The antibacterial activity of the as-prepared samples of RGO and ZnO-RGO nanocomposites against *E.coli* is shown in Fig. 6. Compared to RGO, ZnO-RGO is having better activity. We attribute this to the combined and synergistic effects due to both ZnO and RGO. To ensure the statistical significance of measurement, all assays of RGO and ZnO-RGO were performed in triplicates. Here, data were presented as mean of three experiments. Zone of inhibition of RGO was 18 ± 0.5 mm and for ZnO-RGO it was 28 ± 0.7 mm. It has been reported that both oxidative stress and membrane interactions contribute to the antibacterial activity of graphene-based materials, and direct contact of graphene sheets with cell membrane can lead to cell disruption and death [1]. Most of the works to date have suggested that reactive oxygen species (ROS) generation and consequent oxidative stress are frequently observed with nanoparticle toxicity.

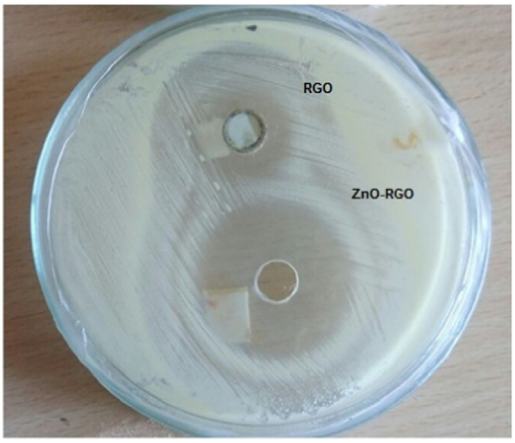

Fig. 6. Antibacterial activity of RGO and ZnO-RGO.

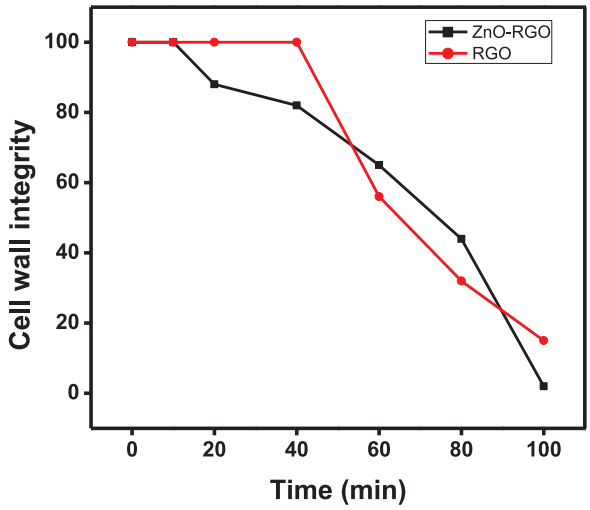

Fig. 7. Cell wall integrity plot for RGO and ZnO-RGO.

3.3. Cell wall integrity using SDS assay

The result of cell wall integrity of ZnO-RGO and RGO using SDS is shown in Fig. 7. From the graph, it is clear that the cell wall integrity gets reduced significantly with increase in time. Once the cell wall is damaged, the cell content reaches out causing cell death. In the present case, we attribute the cell death to the interaction between RGO sheets with bacterial cells. In the case of ZnO-RGO, a sudden decrease in the cell wall integrity was observed immediately after 20 min which can be mainly due to the synergistic effect of ZnO and RGO. Both the physical interactions of graphene layers with the bacterial membranes and the oxidative stress caused by the formation of peroxides facilitated by nano ZnO can be major factors which lead to significant cell death of *E.coli* as we have observed [50].

3.4. AFM image of E.coli

The AFM image of *E.coli* after treating with ZnO-RGO is shown in Fig. 8. The AFM image was helpful in analyzing the effects of ZnO-RGO on bacteria and also observing the surface morphology of *E.coli* after interacting with ZnO-RGO. In its normal form the cell walls of the bacteria are very rigid and the bacteria can grow in a wide range of environmental conditions. From the image, it is clear that the cell walls of *E.coli* get damaged after treating with ZnO-RGO. ZnO-RGO sheets are capable of destroying the rigidity of cell walls of the bacteria by physical wrapping which then induce significant membrane stress on the

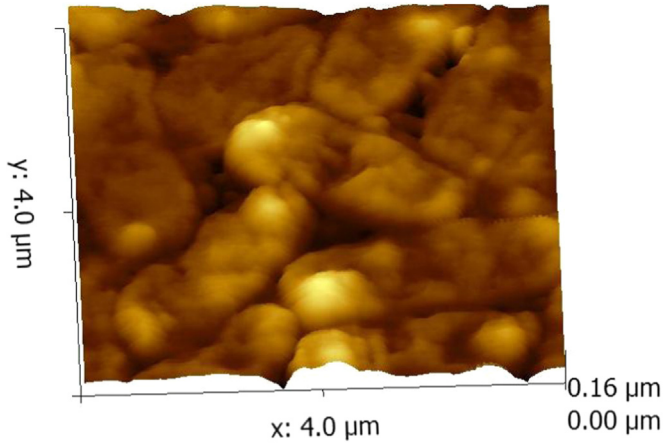

Fig. 8. AFM image of *E.coli* after treating with ZnO-RGO.

surface of the cell walls leading to the death of the bacteria. In a recent study the AFM images obtained by the antibacterial activity of RGO [51], revealed that the actual process of antibacterial activity is associated with the production of nonporous piths on the cell surface causing leakage of intracellular contents confirming our observations.

4. Conclusion

In the present work, we report the synthesis of two forms of graphene derivatives namely, reduced graphene oxide (RGO) through reduction of GO using eco-friendly and abundantly available potato starch and ZnO-decorated/anchored GO (ZnO-RGO). It is seen that in the case of RGO, during the reduction we have carried out some starch components were getting incorporated on the graphene layer which are useful for preventing the aggregation of the layers. We observed that in the case of ZnO-RGO, the reduction of graphene oxide and the conversion of ZnO to nano ZnO occur simultaneously. The detailed characterization of all forms of graphenes (GO and RGO), and ZnO-RGO developed were carried out using FT-IR, XRD, Raman spectra and TEM techniques. The antibacterial activity of RGO and ZnO-RGO was conducted against *E. coli* by well diffusion method. Our results show that ZnO-RGO is more efficient than RGO in their antibacterial properties which we attribute to the synergistic effect of ZnO and RGO towards the bacteria in the nanocomposite. Further, we find that the antibacterial effect of ZnO-RGO towards *E. coli* is due to the disruption of the bacterial cell which could be confirmed by AFM images. The cell wall integrity disruption studies showed the pronounced effect of RGO-ZnO on cell death. Considering the fact that graphene-based materials are less toxic towards mammalian cells, both RGO and ZnO-RGO we have developed can find versatile applications in biomedical field.

Acknowledgements

The authors are grateful to the financial support under DST-FIST (No. 487/DST/FIST/15-16) New Delhi to Sree Sankara College, Kalady.

References

[1] M.D. Rojas-Andrade, G. Chata, D. Rouholiman, J. Liu, C. Saltikov, S. Chen, Antibacterial mechanisms of graphene-based composite nanomaterials, Nanoscale 9 (2017) 994–1006, http://dx.doi.org/10.1039/C6NR08733G.
[2] S.M. Dizaj, A. Mennati, S. Jafari, K. Khezri, K. Adibkia, Antimicrobial activity of carbon-based nanoparticles, Adv. Pharm. Bull. 5 (2015) 19–23, http://dx.doi.org/10.5681/apb.2015.003.
[3] H. Ji, H. Sun, X. Qu, Antibacterial applications of graphene-based nanomaterials: recent achievements and challenges, Adv. Drug Deliv. Rev. 105 (2016) 176–189, http://dx.doi.org/10.1016/j.addr.2016.04.009.
[4] V. Palmieri, M. Carmela Lauriola, G. Ciasca, C. Conti, M. De Spirito, M. Papi, The graphene oxide contradictory effects against human pathogens, Nanotechnology 28 (2017) 152001, http://dx.doi.org/10.1088/1361-6528/aa6150.
[5] B. Sun, J. Wu, S. Cui, H. Zhu, W. An, Q. Fu, C. Shao, A. Yao, B. Chen, D. Shi, In situ synthesis of graphene oxide/gold nanorods theranostic hybrids for efficient tumor computed tomography imaging and photothermal therapy, Nano Res. 10 (2017) 37–48, http://dx.doi.org/10.1007/s12274-016-1264-x.
[6] H. Hashemi, H. Namazi, Sonochemically synthesized blue fluorescent functionalized graphene oxide as a drug delivery system, Ultrason. Sonochem. 42 (2018) 124–133, http://dx.doi.org/10.1016/j.ultsonch.2017.11.010.
[7] X. Fan, Y. Qi, Z. Shi, Y. Lv, Y. Guo, A graphene-based biosensor for detecting microRNA with augmented sensitivity through helicase-assisted signal amplification of hybridization chain reaction, Sens. Actuators B Chem. 255 (2018) 1582–1586, http://dx.doi.org/10.1016/j.snb.2017.08.183.
[8] A.K. Geim, Graphene: status and prospects (80-.), Science 324 (2009) 1530–1534, http://dx.doi.org/10.1126/science.1158877.
[9] A.K. Geim, K.S. Novoselov, The rise of graphene, Nat. Mater. 6 (2007) 183–191, http://dx.doi.org/10.1038/nmat1849.
[10] L. Shi, J. Chen, L. Teng, L. Wang, G. Zhu, S. Liu, Z. Luo, X. Shi, Y. Wang, L. Ren, The antibacterial applications of graphene and its derivatives, Small 12 (2016) 4165–4184, http://dx.doi.org/10.1002/smll.201601841.
[11] M. Yi, Z. Shen, A review on mechanical exfoliation for the scalable production of graphene, J. Mater. Chem. A 3 (2015) 11700–11715, http://dx.doi.org/10.1039/C5TA00252D.
[12] J. Chen, M. Duan, G. Chen, Continuous mechanical exfoliation of graphene sheets via three-roll mill, J. Mater. Chem. 22 (2012) 19625, http://dx.doi.org/10.1039/c2jm33740a.
[13] S. Naghdi, K.Y. Rhee, S.J. Park, A catalytic, catalyst-free, and roll-to-roll production of graphene via chemical vapor deposition: low temperature growth, Carbon N.Y. 127 (2018) 1–12, http://dx.doi.org/10.1016/j.carbon.2017.10.065.
[14] B. Luo, E. Gao, D. Geng, H. Wang, Z. Xu, G. Yu, Etching-controlled growth of graphene by chemical vapor deposition, Chem. Mater. 29 (2017) 1022–1027, http://dx.doi.org/10.1021/acs.chemmater.6b03672.
[15] J. Ning, L. Hao, M. Jin, X. Qiu, Y. Shen, J. Liang, X. Zhang, B. Wang, X. Li, L. Zhi, A facile reduction method for roll-to-roll production of high performance graphene-based transparent conductive films, Adv. Mater. 29 (2017) 1605028, http://dx.doi.org/10.1002/adma.201605028.
[16] X. Ye, Q. Zhou, C. Jia, Z. Tang, Y. Zhu, Z. Wan, Producing large-area, foldable graphene paper from graphite oxide suspensions by in-situ chemical reduction process, Carbon N.Y. 114 (2017) 424–434, http://dx.doi.org/10.1016/j.carbon.2016.11.081.
[17] L. Guo, X. Yin, W. Wu, H. Meng, Preparation of graphene via liquid-phase exfoliation with high gravity technology from edge-oxidized graphite, Colloids Surf. A Physicochem. Eng. Asp. 531 (2017) 25–31, http://dx.doi.org/10.1016/j.colsurfa.2017.07.074.
[18] S.S.A. Shah, H. Nasir, Liquid-phase exfoliation of few-layer graphene and effect of sonication time on concentration of produced few layer graphene, Nano Hybrids Compos. 14 (2017) 17–24, http://dx.doi.org/10.4028/www.scientific.net/NHC.14.17.
[19] S. Szunerits, R. Boukherroub, Antibacterial activity of graphene-based materials, J. Mater. Chem. B 4 (2016) 6892–6912, http://dx.doi.org/10.1039/C6TB01647B.
[20] C. Zhu, S. Guo, Y. Fang, S. Dong, Reducing sugar: new functional molecules for the green synthesis of graphene nanosheets, ACS Nano 4 (2010) 2429–2437, http://dx.doi.org/10.1021/nn102339t.
[21] D.R. Dreyer, S. Murali, Y. Zhu, R.S. Ruoff, C.W. Bielawski, Reduction of graphite oxide using alcohols, J. Mater. Chem. 21 (2011) 3443–3447, http://dx.doi.org/10.1039/C0JM02704A.
[22] M.J. Fernández-Merino, L. Guardia, J.I. Paredes, S. Villar-Rodil, P. Solís-Fernández, A. Martínez-Alonso, J.M.D. Tascón, Vitamin C is an ideal substitute for hydrazine in the reduction of graphene oxide suspensions, J. Phys. Chem. C 114 (2010) 6426–6432, http://dx.doi.org/10.1021/jp100603h.
[23] Y. Wang, Z. Shi, J. Yin, Facile synthesis of soluble graphene via a green reduction of graphene oxide in tea solution and its biocomposites, ACS Appl. Mater. Interfaces 3 (2011) 1127–1133, http://dx.doi.org/10.1021/am1012613.
[24] Z. Fan, W. Kai, J. Yan, T. Wei, L. Zhi, J. Feng, Y. Ren, P. Song, F. Wei, Facile synthesis of graphene nanosheets via Fe reduction of exfoliated graphite oxide, ACS Nano 5 (2011) 191–198.
[25] G. Du, Y. Li, L. Zhang, X. Wang, P. Liu, Y. Feng, X. Sun, Facile self-assembly of honeycomb ZnO particles decorated reduced graphene oxide, Mater. Lett. 128 (2014) 242–244, http://dx.doi.org/10.1016/j.matlet.2014.04.126.
[26] G. Du, X. Wang, L. Zhang, Y. Feng, Y. Li, Controllable synthesis of different ZnO architectures decorated reduced graphene oxidenanocomposites, Mater. Lett. 96 (2013) 128–130, http://dx.doi.org/10.1016/j.matlet.2013.01.063.
[27] Z.U. Abideen, H.W. Kim, S.S. Kim, An ultra-sensitive hydrogen gas sensor using reduced graphene oxide-loaded ZnO nanofibers, Chem. Commun. 51 (2015) 15418–15421, http://dx.doi.org/10.1039/C5CC05370F.
[28] R. Atchudan, T.N.J.I. Edison, S. Perumal, D. Karthikeyan, Y.R. Lee, Facile synthesis of zinc oxide nanoparticles decorated graphene oxide composite via simple solvothermal route and their photocatalytic activity on methylene blue degradation, J. Photochem. Photobiol. B Biol. 162 (2016) 500–510, http://dx.doi.org/10.1016/j.jphotobiol.2016.07.019.
[29] R.S. Rajaura, V. Sharma, R.S. Ronin, D.K. Gupta, S. Srivastava, K. Agrawal, Y.K. Vijay, Synthesis, characterization and enhanced antimicrobial activity of reduced graphene oxide–zinc oxide nanocomposite, Mater. Res. Express 4 (2017) 25401, http://dx.doi.org/10.1088/2053-1591/aa5bff.
[30] W. Hu, C. Peng, W. Luo, M. Lv, X. Li, D. Li, Q. Huang, C. Fan, Graphene-based antibacterial paper, ACS Nano 4 (2010) 4317–4323, http://dx.doi.org/10.1021/nn101097v.
[31] S.S. Nanda, D.K. Yi, K. Kim, Study of antibacterial mechanism of graphene oxide

using Raman spectroscopy, Sci. Rep. 6 (2016) 28443, http://dx.doi.org/10.1038/srep28443.
[32] S. Liu, T.H. Zeng, M. Hofmann, E. Burcombe, J. Wei, R. Jiang, J.C. Kong, Y. Chen, Antibacterial activity of graphite, graphite oxide, graphene oxide, and reduced graphene oxide: membrane and oxidative stress, ACS Nano 5 (2011) 6971–6980, http://dx.doi.org/10.1021/nn202451x.
[33] K. Krishnamoorthy, N. Umasuthan, R. Mohan, J. Lee, S.-J. Kim, Antibacterial Activity of Graphene Oxide Nanosheets, Sci. Adv. Mater. 4 (2012) 1111–1117, http://dx.doi.org/10.1166/sam.2012.1402.
[34] S. Kellici, J. Acord, J. Ball, H.S. Reehal, D. Morgan, B. Saha, A single rapid route for the synthesis of reduced graphene oxide with antibacterial activities, RSC Adv. 4 (2014) 14858, http://dx.doi.org/10.1039/c3ra47573e.
[35] G.R. Navale, C.S. Rout, K.N. Gohil, M.S. Dharne, D.J. Late, S.S. Shinde, Oxidative and membrane stress-mediated antibacterial activity of WS2 and rGO2 nanosheets, RSC Adv. 5 (2015) 74726–74733, http://dx.doi.org/10.1039/c5ra15652a.
[36] K. Ravichandran, K. Nithiyadevi, B. Sakthivel, T. Arun, E. Sindhuja, G. Muruganandam, Synthesis of ZnO:Co/rGO nanocomposites for enhanced photocatalytic and antibacterial activities, Ceram. Int. 42 (2016) 17539–17550, http://dx.doi.org/10.1016/j.ceramint.2016.08.067.
[37] W.S. Hummers, R.E. Offeman, Preparation of graphitic oxide, J. Am. Chem. Soc. 80 (1958) 1339, http://dx.doi.org/10.1021/ja01539a017.
[38] Y. Feng, N. Feng, G. Du, A green reduction of graphene oxide via starch-based materials, RSC Adv. 3 (2013) 21466, http://dx.doi.org/10.1039/c3ra43025a.
[39] M.Q. Yang, Y.J. Xu, Basic principles for observing the photosensitizer role of graphene in the graphene-semiconductor composite photocatalyst from a case study on graphene-ZnO, Electroanalysis 28 (2016) 2237–2244.
[40] C.-N. Lok, C.-M. Ho, R. Chen, Q.-Y. He, W.-Y. Yu, H. Sun, P.K.-H. Tam, J.-F. Chiu, C.-M. Che, Silver nanoparticles: partial oxidation and antibacterial activities, J. Phys. Chem. C 117 (2013) 21724–21734, http://dx.doi.org/10.1021/jp408400c.
[41] S. Yongchao, T. Samulski Edward, Synthesis of water soluble graphene, Nano Lett. 8 (2008) 1679–1682, http://dx.doi.org/10.1021/nl080604h.
[42] M.K. Kavitha, H. John, P. Gopinath, R. Philip, Synthesis of reduced graphene oxide–ZnO hybrid with enhanced optical limiting properties, J. Mater. Chem. C 1 (2013) 3669, http://dx.doi.org/10.1039/c3tc30323c.
[43] M.I. Ali Umar, C.C. Yap, R. Awang, M.H. Hj Jumali, M. Mat Salleh, M. Yahaya, Characterization of multilayer graphene prepared from short-time processed graphite oxide flake, J. Mater. Sci. Mater. Electron. 24 (2013) 1282–1286, http://dx.doi.org/10.1007/s10854-012-0920-5.
[44] S. Sadhukhan, T.K. Ghosh, D. Rana, I. Roy, A. Bhattacharyya, G. Sarkar, M. Chakraborty, D. Chattopadhyay, Studies on synthesis of reduced graphene oxide (RGO) via green route and its electrical property, Mater. Res. Bull. 79 (2016) 41–51, http://dx.doi.org/10.1016/j.materresbull.2016.02.039.
[45] Z. Bo, X. Shuai, S. Mao, H. Yang, J. Qian, J. Chen, J. Yan, K. Cen, Green preparation of reduced graphene oxide for sensing and energy storage applications, Sci. Rep. 4 (2014) 1–8, http://dx.doi.org/10.1038/srep04684.
[46] R. Atchudan, T.N.J.I. Edison, S. Perumal, D. Karthikeyan, Y.R. Lee, Facile synthesis of zinc oxide nanoparticles decorated graphene oxide composite via simple solvothermal route and their photocatalytic activity on methylene blue degradation, J. Photochem. Photobiol. B Biol. 162 (2016) 500–510, http://dx.doi.org/10.1016/j.jphotobiol.2016.07.019.
[47] K. Thiyagarajan, M. Muralidharan, K. Sivakumar, Interfacial ferromagnetism in reduced graphene oxide–ZnO nanocomposites, J. Mater. Sci. Mater. Electron (2018), http://dx.doi.org/10.1007/s10854-018-8735-7.
[48] M. Jeyavelan, A. Ramesh, R. Rathes Kannan, T. Sonia, K. Rugunandhiri, M.S.L. Hudson, Facile synthesis of uniformly dispersed ZnO nanoparticles on a polystyrene/rGO matrix and its superior electrical conductivity and photocurrent generation, RSC Adv. 7 (2017) 31272–31280, http://dx.doi.org/10.1039/C7RA04361A.
[49] Y. Liu, Y. Hu, M. Zhou, H. Qian, X. Hu, Microwave-assisted non-aqueous route to deposit well-dispersed ZnO nanocrystals on reduced graphene oxide sheets with improved photoactivity for the decolorization of dyes under visible light, Appl. Catal. B Environ. 125 (2012) 425–431, http://dx.doi.org/10.1016/j.apcatb.2012.06.016.
[50] T. Kavitha, A.I. Gopalan, K.P. Lee, S.Y. Park, Glucose sensing, photocatalytic and antibacterial properties of graphene-ZnO nanoparticle hybrids, Carbon N.Y. 50 (2012) 2994–3000, http://dx.doi.org/10.1016/j.carbon.2012.02.082.
[51] S. Yaragalla, R. Rajendran, J. Jose, M.A. Almaadeed, N. Kalarikkal, S. Thomas, Preparation and characterization of green graphene using grape seed extract for bioapplications, Mater. Sci. Eng. C 65 (2016) 345–353, http://dx.doi.org/10.1016/j.msec. 2016.04.050.